Compensation of Vehicle Motion Influence in a Long Baseline System Field Trial

Zhao Li[1,2,3], Stan E. Dosso[3], Dajun Sun[1,2]
1 Science and Technology on Underwater Acoustic Laboratory, Harbin Engineering University, China;
2 College of Underwater Acoustic Engineering, Harbin Engineering University, China;
3 School of Earth and Ocean Sciences, University of Victoria, Canada.
E-mail: lizhao0517@sina.cn

***Abstract* — This paper develops a method to compensate for vehicle motion during the interrogation-reception time interval between the vehicle and transponders in a long baseline (LBL) system, and evaluates the results in lake trials. The compensation method is based on Bayesian inversion which includes travel-time corrections as additional unknown parameters with prior estimates determined by interpolating the vehicle location at interrogation times from the results of a preliminary inversion using a static-vehicle model (SM). The lake trials show that average acoustic localization errors for a surface vehicle were reduced from 19 ± 14 cm error for the SM inversion to 3.4 ± 1.4 cm for the motion-compensated inversion (MM)**

Keywords — underwater acoustic localization, vehicle motion compensation, travel-time correction, Bayesian inversion.

I. Introduction

The localization error of the long baseline (LBL) acoustic localization system is sensitive to vehicle motion between the time the vehicle sends out an interrogation signal and the times of reception at the vehicle of the acoustic replies from the various transponders. However, the static-vehicle model (SM) for localization does not take vehicle motion into consideration and assumes that the one-way acoustic travel time from a transponder to the vehicle is simply half of the observed two-way travel-time from vehicle to transponder and back [1][2]. This can result in significant errors in localizing a moving vehicle. One solution for this problem is to localize vehicles using one-way travel-times rather than two-way travel-times, which can be achieved either by synchronizing the transponders with transceiver [3] or adding a precise-located surface ship [4]. Kalman filter (KF) can be used to compensate for motion during localization via motion modeling [5][6], but our curiosity is if this problem can be addressed using two-way acoustic timing measurements only without KF approach.

In this paper, the SM is extended to address localization errors caused by vehicle motion. Vehicle interrogation coordinates, transponder coordinates, and time corrections are all estimated via linearized Bayesian inversion, given reasonable prior information. This paper describes the application of the motion-compensated model (MM) in a LBL field trial. The comparison of localization results between the two methods indicate the MM approach is effective in compensating the influence of vehicle motion .

This paper is funded by the National High Technology Research and Development Program 2012AA091401.

II. LBL Trial Procedure

On November 3rd, 2014, a trial was carried out in Songhua lake, Jilin, China, to test a LBL acoustic localization system. This lake is an artificial reservoir formed by the dam of Fengman hydropower station. The average water depth was about 45 m during the trial period. In the trial, a surface boat was used as a substitute for an AUV, and localized by both LBL and GPS system. GPS data were logged as references to evaluate the acoustic localization accuracy. The trial includes transponders deployment, array element localization (AEL) for the transponders, maneuvering vehicle localization (MVL) survey and transponders recovery.

A. LBL Acoustic Localization System

The LBL includes four transponders marked from T1 to T4 and a transceiver, all designed by Harbin Engineering University. The transceiver is composed of an acoustic transducer, a signal processing box, a power box, a computer and cables, shown in Fig. 1. The system works at 8-16 kHz frequency with 190 dB source level. Every 2 s, the transceiver interrogates transponders with a 10 ms linear frequency modulation signal (upchirp). Each transponder replies with a individual frequency hopping signal after a specific turn-around time. The feature of this system is there are two optional signal sampling rates, 40 kHz and 200 kHz , in the transceiver.

Fig. 1. Components of the LBL system tested in the field trial, including transducer, transponder, computer, signal processing box and power box (counter-clockwise from top left).

978-0-933957-43-5 ©2015 MTS

Transponders were deployed on the lake bed with a "float–cord–sinker" mooring. The components of the mooring is as follows (from bottom to top): 30 kg sinker, 8 m cord, transponder, 2 m cord and floats. The processing and power boxes of the transceiver and a computer were placed inside a 7 m long boat used as the trial platform. The acoustic transducer of the transceiver was firmly installed on the broadside by a 4.5 m long triangular-prism-shaped steel frame. The depth of the transducer was about 3.9 m when the frame was vertically fixed on the boat.

B. GPS and Gyroscpoe

The antenna of Leica GPS1200 mobile station was fastened on top of the steel fame and was set in the real time kinematic (RTK) mode. The GPS base station was set on the roof of the highest building of a holiday village on the lakeside with a less than 1 km baseline. An Octans gyroscope from IxBlue was installed between the frame and the transducer to measure yaw, pitch and roll of the boat during the trial, shown as Fig. 2. The GPS output pulse per second (PPS) was used as trigger of the LBL system to interrogate transponders and log GPS and gyroscope data.

The distance between the GPS antenna and the transducer, defined in an established boat coordinate system, was measured after installation. With this distance and the data from GPS and gyroscope, the geodetic coordinates of the transducer can be calculated using the method established in [7]. In this lake trial, the distance between the GPS antenna and the transducer was measured as [8.5, 0.8, 591.0] cm. Gyroscope precision is 0.01 degree, and localization precision is within 2 cm by RTK GPS. Further considering the vibration and bending of the steel frame during survey, the final uncertainty of the calculated transducer coordinates was thought to be smaller than 4 cm.

C. AEL and MVL Survey

After the deployment of transponders, SSP, shown as Fig. 3, was measured by a sound velocity probe.

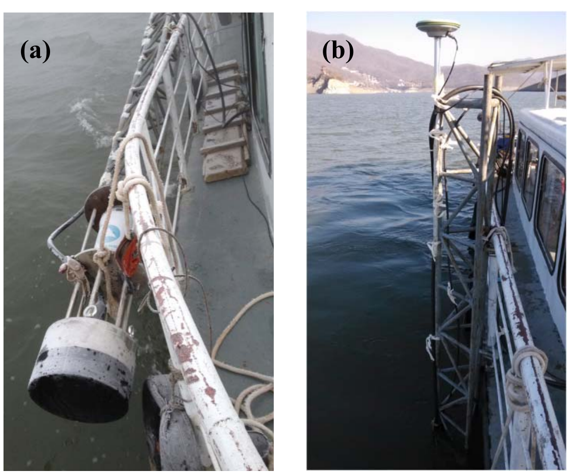

Fig. 2. The installation of (a) transducer, gyroscope and (b) GPS antenna. The acoustic transducer of the transceiver was firmly installed on the broadside by a steel frame. A gyroscope was installed between the frame and the transducer. A GPS antenna was fixed firmly on top of the fame.

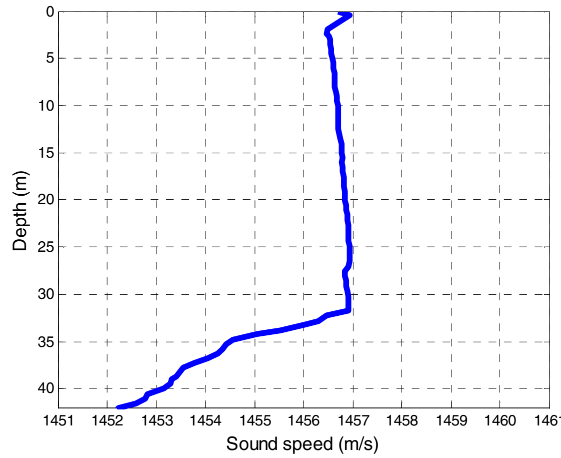

Fig. 3. Sound speed profile measured in the lake trial.

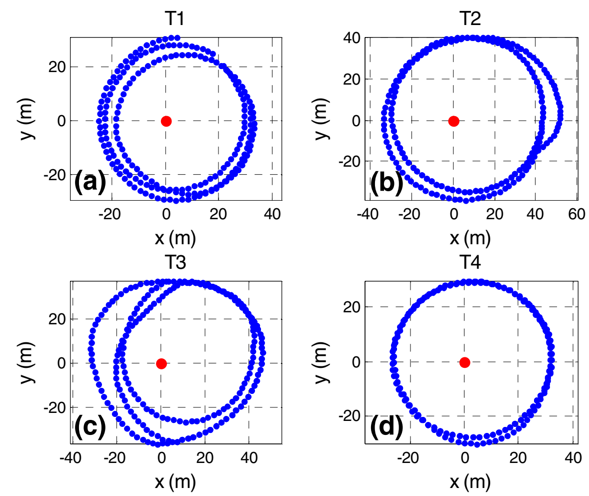

Fig. 4. AEL tracks of each transponder in the trial. The blue dots represet the AEL survey tracks of the boat. The red dots from (a) to (d) are the transponder T1 to T4. The origin (0,0) of each panel represents the transponder location.

The AEL survey was carried out to locate geodetic coordinates of each transponder. During the AEL survey, each transponder was interrogated by the LBL transceiver along three circular tracks of about 40 m radius centered on the surface floats. In order to locate the transponder precisely, the sample rate of the transceiver was set as 200 kHz. When the signal to noise ratio (SNR) is high, this sample rate can provide about 5 μs timing precision. The tracks of AEL survey are shown in Fig. 4.

When AEL survey was finished, the boat was treated as a substitute for an AUV, and moved back and forth within an about 300 m × 300 m area centered on the average of transponders coordinates. The geometry of the transponder array and the survey tracks are shown in Fig. 5. During this maneuvering vehicle localization (MVL) survey, the boat speed was controlled around 1.5 m/s. The transceiver signal sample rate was set to 40 kHz to ensure all four transponder signals can be processed on-site by the signal processing box.

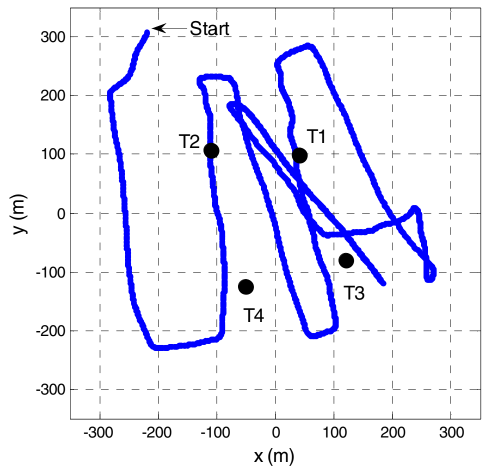

Fig. 5. Transducer track and transponders array geometry in geodetic coordinate. Transducer tracks calculated with GPS and gyroscope data are plotted in blue lines. The four solid black circles are four transponder (T1 - T4) locations estimated by the AEL survey. The MVL survey started from the up left of this figure.

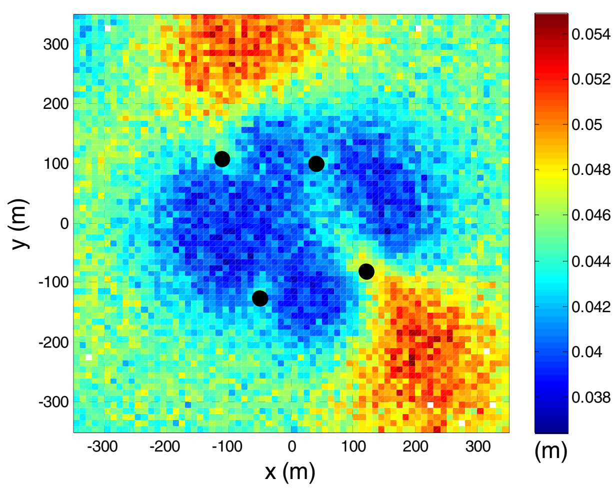

Fig. 6. Horizontal RMS localization errors over the test range. The color in each pixel of the figure represents localization error in the corresponding vehicle location. The four black circles show the transponder locations.

Using the geometry of the transponder array, the measured SSP and the prior uncertainty of the travel-time and transponders locations, a 1000 realizations Monte Carlo simulation was carried out to evaluate the expected localization accuracy. In the simulation, measured transponder locations and SSP are used as true values and the vehicle is assumed to be stable during the interrogation-reception time interval. Gaussian distributed random timing errors of standard deviation 30 μs are added to the travel-times calculated by ray tracing. 0.02 m and 0.1 m/s bias are introduced to transponder locations and SSP, respectively. The root mean square (RMS) localization errors of the SM over the test range are presented in Fig. 6, which are much smaller than the localization error in the field data processing results (shown in Section IV). These differences in localization errors indicate the effect of the vehicle motion that need to be compensated if higher localization accuracy is required.

III. Data Processing Methods

In the static localization model, the differences in interrogation and reception coordinates of a maneuvering vehicle are ignored and the "observed" one-way travel-times simply halved by the measured two-way travel-times are not obtained accurately. In this paper, this problem is addressed by using travel-time corrections to compensate the time difference between interrogation and reception. Considering the replied signals are not received at the same coordinates, so only interrogation coordinates are localized in this paper.

In the MM method, the dependence of ship location $(x,y,z)^{\mathrm{T}}$, transponder location $(X,Y,Z)^{\mathrm{T}}$ and the observed one-way travel-time t^{obs} can be written as

$$t\left(x_i,y_i,z_i,X_j,Y_j,Z_j,c\right)+\Delta t_{ij}=t_{ij}^{\mathrm{obs}} \quad , \qquad (1)$$

where Δt is the travel-time correction, which compensates the signal travel-time differences of receiving and interrogation. The sequence number of the localization cycle is marked as i and j represents different transponders. The modeled one-way travel time t is calculated with interrogation location, transponder location and SSP c via ray tracing method.

As presented in [1], [8] and [9], with a local linearization and formulation in terms of the model parameter rather than the model perturbation, the maximum a *posteriori* (MAP) solution of the model parameters, $\mathbf{m}$, can be expressed as

$$\mathbf{m}=\hat{\mathbf{m}}+\left(\mathbf{J}^{\mathrm{T}}\mathbf{C}_D^{-1}\mathbf{J}+\mathbf{C}_M^{-1}\right)^{-1}\mathbf{J}^{\mathrm{T}}\mathbf{C}_D^{-1}\left(\mathbf{d}\text{-}\mathbf{J}\hat{\mathbf{m}}\right), \qquad (2)$$

where $\mathbf{m}=\left[x_i,y_i,z_i,X_j,Y_j,Z_j,\Delta t_{ij}\right]^{\mathrm{T}}$ is the unknown model parameters vector in this problem. $\mathbf{J}$ represents the Jacobian matrix consisted by the partial derivatives of t with respect to $\mathbf{m}$. $\mathbf{C}_D$ is the covariance matrix of the data, $\mathbf{C}_M$ is the covariance matrix of the prior model.

Due to underdetermine issue in this inversion, priors play important roles to ensure a stable solution, and must be chosen reasonably. In this paper, the inversion results of the SM are used to calculate the prior of this MM method.

Assume the one-way travel-time from the transceiver to a transponder is t^{I} and the prior of the travel-time corrections can be expressed as the difference between the observed and actual travel-times.

$$\Delta\hat{t}=t^{\mathrm{obs}}-t^{\mathrm{I}}, \qquad (3)$$

where t^{I} is calculated with $\hat{\mathbf{X}}$, the priors for unknown interrogation locations, and transponders locations using ray-tracing method. $\hat{\mathbf{X}}$ are obtained by interpolating the static model inversion results with time instants. In this paper, the SM results of current cycle and last three cycles are used to interpolate $\hat{\mathbf{X}}$.

The halved two-way travel-time t_{ij}^{obs} of the i^{th} localization cycle (current cycle) can be approximately treated as received at the time instant $(i-1)\tau+t_{ij}^{\mathrm{obs}}$ when the vehicle reaches to the SM localization result $\mathbf{X}_i^{\mathrm{st}}$, where τ is cycle period of the localization system. Thus, coordinates in $\mathbf{X}_i^{\mathrm{st}}$ corresponds to the instant $(i-1)\tau+t_{ij}^{\mathrm{obs}}$ and the similar relationship can be established in the last three cycles. With cubic spline interpolation, curves of $\mathbf{X}^{\mathrm{st}}$ versus instants is obtained. The vehicle location at any time instant from $(i-4)\tau+t_{(i-3)j}^{\mathrm{obs}}$ to $(i-1)\tau+t_{ij}^{\mathrm{obs}}$ can be interpolated by these curves. So given instant $(i-1)\tau$, $\mathbf{X}_{ij}^{\mathrm{Int}}$, interpolated vehicle coordinates in i^{th} cycle are calculated. This procedure is repeated for each transponder, and $\hat{\mathbf{X}}_i$ is set as the average of the $\mathbf{X}_{ij}^{\mathrm{Int}}$. Finally, t^{I} is calculated with $\hat{\mathbf{X}}$ and transponders locations using ray tracing.

IV. Field Trial Results

Both array element localization (AEL) survey and maneuvering vehicle localization (MVL) survey results are shown in this section. The results of the SM and MM are compared to show the effect of introducing travel-time corrections into the localization.

A. AEL Survey Results

The circular track for AEL was repeated three times, and hence three sets of data were recorded in total for each transponder. The observed data in each circular track were processed separately to locate the transponder. The estimated horizontal location of each transponder is shown in Fig. 7(a) - (d). The black circles in the figure are the 95% confidence regions of each localization result estimated from posterior covariance matrix. The larger posterior uncertainty of T3 is probably caused by more unsymmetrical tracks for this observation during the survey. Fig. 7(e) shows the time residuals of each transponder. Most of the residuals are within 20 μs, higher than the expected timing precision due to the transceiver locations errors. According to the AEL posterior uncertainty and residuals in Fig. 7, it is reasonable to consider the precision of transponder location is better than 4 cm. The averages of the three estimated locations for each transponder are used as the prior estimates in the MVL.

B. MVL Survey Results

The maneuvering surface boat is localized with two models: the static model (SM) that estimates vehicle and transponder locations ignoring vehicle motion; the motion-compensated model (MM) that estimates these locations and travel-time corrections. In this paper, localization errors in the trial are regarded as the difference between inversion results and the measured geodetic coordinates of the transducer. Fig. 8 is the localization results of SM and MM presented with LBL transceiver track measured by GPS. The gaps in the estimated tracks in Fig. 8 are caused by failure in signal detection due to the low SNR caused by signal overlapping, strong multipath and surface reverberation.

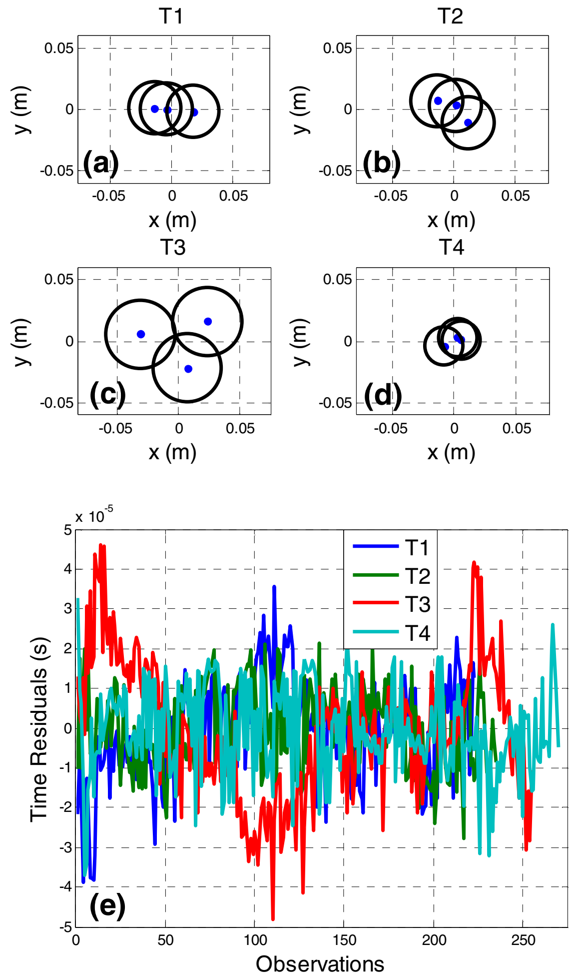

Fig. 7. Estimated transponder locations and time residuals. From (a) to (d), the three blue dots in each subgraph are calculated coordinates of transponder from T1 to T4. The black circles in the figure represent the 95% confidence region of each localization result. (e) is the time residuals of the AEL inversion. Four colors represent residuals of each transponder.

In Fig. 8, the estimated tracks of two methods are both in accordance with the measured transducer locations. Further check is carried out by displaying the localization error curves versus time, shown in Fig. 9. The error of SM method varies significantly. The lowest accuracy is almost 1 m at the beginning. Generally, large localization errors correspond to places where the boat is outside the transponder array. When the vehicle was inside the array, the maximum localization error is about 50 cm and the average localization error is calculated to be 19±14 cm. With motion-compensated inversion, the localization errors are much smaller. The lowest localization error is obtained using the MM method with an average error of 3.4±1.4 cm when the vehicle was inside the transponder array. Even when the vehicle moved outside the array, the error is still generally less than 20 cm.

The improvement in the localization result is also indicated

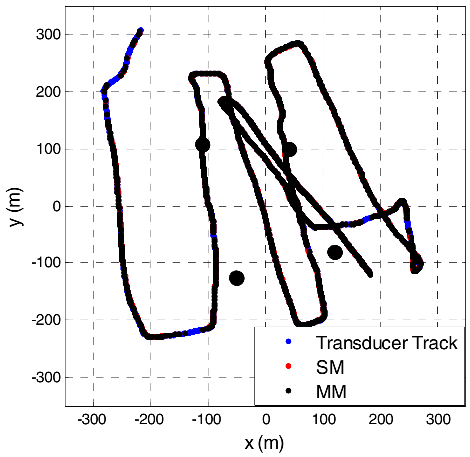

Fig. 8. Localized transceiver coordinates with different models. Vehicle inversion results are presented in dots with different colors. Good inversion results make these dots seem to overlap each other when looking in large scale. Four solid black circles are transponder locations.

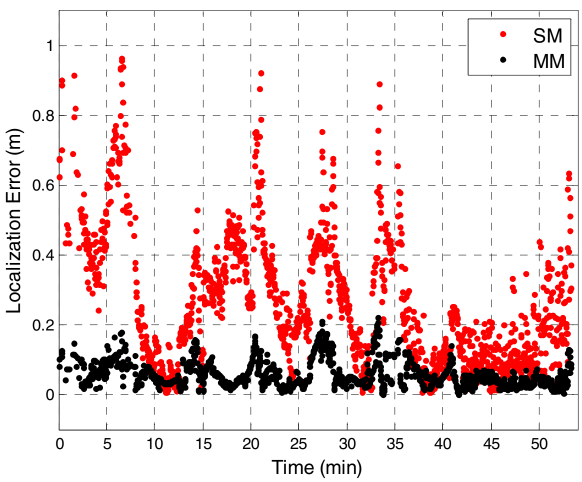

Fig. 9. Localization errors of different methods. Red dots are the errors of the static model (SM). Black dots represent the errors of the motion-compensated model (MM).

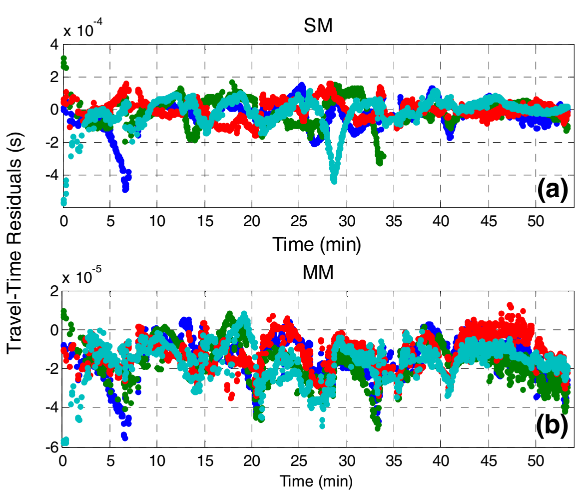

Fig. 10. Travel-time residuals of the (a) SM and (b) MM methods.

in the travel-time residuals. Before travel-times are corrected (SM), the time residuals vary from -400 μs to 200 μs, which is much larger than the 25 μs timing precision estimated by sample rate. In the MM method, however, around 40 μs level residuals show that the data are better fitted.

V. SUMMARY

Long baseline acoustic localization systems are found susceptible to errors for maneuvering vehicles due to vehicle motion between the time the vehicle sends out an interrogation signal and the times of reception for the acoustic replies from the various transponders in lake trial. To address this problem, in this paper, a motion-compensated model for vehicle localization is developed which includes travel-time corrections for all receptions as unknown parameters in a ray-based linearized inversion algorithm. The key to this algorithm is setting the prior estimates for the travel-time corrections. This is carried out here by first estimating the vehicle locations at the time instants the interrogation signals are sent by applying cubic-spline interpolation of the results of an initial localization inversion assuming a static vehicle, and then determining the corresponding travel-times by ray tracing. With this new method, the averaged localization errors are decreased to 3.4±1.4 cm within the transponder array. This is about the same level of accuracy as the GPS-based transceiver locations, which are considered the reference.

REFERENCES

[1] D. Thomson, and S. E. Dosso, “AUV localization in an underwater acoustic positioning system”, *MTS/IEEE OCEANS - Bergen*, 2013.

[2] P. Newman and J. Leonard, “Pure range-only sub-sea SLAM,” in *Proc. IEEE/Interoational Conference on Robotics and Automation*, Taipei, Taiwan, 2003, pp. 1921-1926.

[3] S. E. Webster, R. M. Eustice, H. Singh, and L. L. Whitcomb, "Advances in single-beacon one-way-travel-time acoustic navigation for underwater vehicles," *Inter. J. Robot Res*., vol. 31, no. 8, pp. 935–949, Jun. 2012.

[4] N. Kussat, D, Chadwell, and R, Zimmerman, “Absolute Positioning of an Autonomous Underwater Vehicle Using GPS and Acoustic Measurements”, *IEEE Journal of Oceanic Engineering*, vol, 30, pp. 153–164, 2005.

[5] L. Paull, S. Saeedi, M. Seto, and H. Li,. “AUV Navigation and Localization: A Review”, *IEEE Journal of Oceanic Engineering*, vol, 39, pp. 131–149, 2014.

[6] A. Bahr, J. J. Leonard, and M. F. Fallon, “Cooperative localization for autonomous underwater vehicles”. Inter. J. Robot Res., vol. 28, no. 6, pp. 714–728, Jun. 2009

[7] M. Yu, “In-situ calibration of transceiver alignment for a high-precision USBL system,” in Proc. IEEE/International Conference on Computer Application and System Modeling, Taiyuan, China, 2010, pp. 84-87.

[8] S. E. Dosso, M. Fallat, B. Sotirin, and J. Newton, “Array element localization for horizontal arrays via Occam’s inversion”, *The Journal of the Acoustical Society of America*, vol,104, pp. 846–859, 1998.

[9] S. E. Dosso, and G. R. Ebbeson, “Array element localization accuracy and survey design”, *Canadian Acoustics*, vol, 34, pp. 1–11, 2006.

[10] R. C. Aster, B. Borchers, C. H. Thurber, “Parameter Estimation and Inverse Problems”, *Academic Press*: MA USA, pp. 253-269.